INTERNATIONAL JOURNAL FOR NUMERICAL METHODS IN FLUIDS
Int. J. Numer. Meth. Fluids 2001; **35**: 319–340

On the efficiency of semi-implicit and semi-Lagrangian spectral methods for the calculation of incompressible flows

Chuanju Xu[a,1] and Richard Pasquetti[b,*,2]

[a] *Department of Mathematics, Xiamen University, Xiamen 361005, Fujian, People's Republic of China*
[b] *Laboratoire J.A. Dieudonné, UMR CNRS 6621, Université de Nice-Sophia Antipolis, Nice, France*

SUMMARY

Classical semi-implicit backward Euler/Adams–Bashforth time discretizations of the Navier–Stokes equations induce, for high-Reynolds number flows, severe restrictions on the time step. Such restrictions can be relaxed by using semi-Lagrangian schemes essentially based on splitting the full problem into an explicit transport step and an implicit diffusion step. In comparison with the standard characteristics method, the semi-Lagrangian method has the advantage of being much less CPU time consuming where spectral methods are concerned. This paper is devoted to the comparison of the 'semi-implicit' and 'semi-Lagrangian' approaches, in terms of stability, accuracy and computational efficiency. Numerical results on the advection equation, Burger's equation and finally two- and three-dimensional Navier–Stokes equations, using spectral elements or a collocation method, are provided. Copyright © 2001 John Wiley & Sons, Ltd.

KEY WORDS: characteristics method; high-Reynolds number flows; Navier–Stokes equations; semi-Lagrangian methods; spectral methods

1. INTRODUCTION

In spectral simulations of incompressible viscous flows, the linear terms are often treated implicitly and the non-linear convective term explicitly, to obtain a linear system in space after the time discretization. However, such semi-implicit treatments have generally severe stability restrictions on the time step when high-Reynolds number flows are computed. Another popular approach for the treatment of the convective term is the characteristics method (see, for example, References [1–4]), sometimes termed as 'transport + diffusion algorithm'. It

* Correspondence to: Laboratoire J.A. Dieudonné, UMR CNRS 6621, Université de Nice-Sophia Antipolis, 06108 Nice, France.
[1] E-mail: cjxu@xmu.edu.cn
[2] E-mail: richard.pasquetti@unice.fr

Received August 1999
Revised February 2000

consists of splitting the computation at each time step into two steps: transport of the previous solution on the characteristics and resolution of Stokes-like equations or diffusion-like equations, e.g. in the framework of projection methods. The characteristics method, which makes use of direct approximations of the material derivatives, was first introduced in the finite element framework (see above mentioned references). Adaptation of such an approach to the spectral methods are more recent [5]. Theoretically, if a backward differentiation scheme is applied, the characteristics method is an unconditionally stable numerical procedure. As a result, large time steps can be used in the computations.

However, some difficulties remain, especially when high-order spatial approximations are involved. First, a difficulty arises from the location of the feet of the characteristics and from the evaluation of the solution at these points: to retain high-order accuracy, high-order Lagrange interpolants have to be used, which is expensive in terms of CPU time. Second, if the spatial discretization is based on a multi-domain or spectral element method, it may be necessary to trace back the characteristics over several sub-domains or elements. This can introduce additional errors and furthermore affect the total stability property of the scheme. Third, no general effective theoretical results are available concerning the analysis of stability and convergence of the characteristics method, as soon as the transport step is only solved approximatively.

An alternative method, also based on the splitting transport step–diffusion step but avoiding the costly interpolations required for the solution evaluations at the feet of the characteristics, is to use a semi-Lagrangian approach. Such a method can be recast in the general integration factor splitting scheme generator introduced in Reference [6]. It consists of determining the transport of the previous solution on the characteristics via solving an advection equation with appropriate sub-time discretization. The aim of this paper is to verify the properties of the resulting algorithm, for different problems and using different spectral approaches, in terms of stability, accuracy and also computational efficiency, with comparisons with standard semi-implicit schemes.

In the first part of the paper (Sections 2–4), the semi-Lagrangian method is introduced, a few illustrating schemes are described and the sensitive point of the boundary conditions for the transport step is discussed. Then we give detailed comparisons on the stability and accuracy between the semi-Lagrangian and semi-implicit schemes. These comparisons are first performed on one-dimensional problems (Burger's and advection–diffusion equations), then for the two-dimensional regularized driven cavity problem, using a spectral element method, and finally for a three-dimensional cavity problem, using a Chebyshev collocation method. For this latter test, we also compare the efficiency of the two different approaches in terms of CPU time with justification of the results by operation counts.

The main notations used in the paper are the following:

- $u(x, t)$: exact solution u at the point x and time t
- u^n: numerical approximation of u at time $t = t^n$
- $\chi(x, t;\ \tau),\ 0 \leq \tau \leq t$: characteristics equation
- $\tilde{u}$: $\tilde{u}(x, t;\ \tau) := u(\chi(x, t;\ \tau), \tau)$
- $\tilde{u}^n$: approximation of $\tilde{u}$ at time $\tau = t^n$, with $t = t^{n+1}$
- $\bar{u}$: exact solution of each transport equation solved at each time cycle
- $\bar{u}^m$: approximation of $\bar{u}$ at sub-time cycle m

2. THE SEMI-LAGRANGIAN METHOD

For the sake of simplicity, we consider the standard advection–diffusion problem: given v, $\mathbf{v}$ and f, find u such that

$$\frac{\partial u}{\partial t} + \mathbf{v}\cdot\nabla u - v\Delta u = f, \quad x\in\Omega, \quad 0 < t < T \tag{1}$$

completed with appropriate initial and boundary conditions. Here $\Omega \subset R^d$ $(d = 1, 2, 3)$, $\mathbf{v} = (v_1, \ldots, v_d)$ is a velocity field and v is a positive constant diffusion coefficient.

Equation (1) can be rewritten in the form

$$\frac{\mathrm{D}u}{\mathrm{D}t} - v\Delta u = f \tag{2}$$

where $\mathrm{D}/\mathrm{D}t$ is the material (Lagrangian) derivative, i.e. the total derivative in the streamline direction $\mathbf{v}$. The basic idea of the classical characteristics method consists in the discretization of Equation (2), rather than Equation (1). For example, using the first-order backward Euler (BE1) difference scheme, one obtains

$$\frac{1}{\Delta t}u^{n+1} - v\Delta u^{n+1} = f^{n+1} + \frac{1}{\Delta t}u^n(\chi(x, t^{n+1};\ t^n)) \tag{3}$$

where Δt is the time step, n is the time cycle index and $\chi(x, t;\ \tau)$ is the solution of the characteristics equation

$$\begin{cases} \dfrac{\mathrm{d}\chi}{\mathrm{d}\tau} = \mathbf{v}(\chi, \tau), \quad 0 < \tau < t \\ \chi(x, t;\ t) = x \end{cases} \tag{4}$$

which defines the trajectory of the particle that reaches the position x at time t.

After the spatial discretization, for each collocation point the classical characteristics method consists of the following two steps:

(i) location of the foot of the characteristic;
(ii) evaluation of u^n at this point.

Such a procedure is clearly expensive and, moreover, may be unstable when high-order approximations are concerned, such as spectral, spectral elements or h–p finite element methods.

The semi-Lagrangian approach appears to be able to preserve the main advantages of the characteristics method together with being less expensive in computational time. As shown hereafter, for the advection–diffusion equation it is also based on the splitting transport step–diffusion step.

To be more general than in Equation (3), let us introduce the backward Euler approximation of order Q (BEQ) of Equation (2). Considering the Q consecutive time instants $t^{n+1-q} = t^{n+1} - q\Delta t,\ q = 1, \ldots, Q$, then we have

$$\frac{\alpha_0 u^{n+1} + \alpha_1 \tilde{u}^n + \cdots + \alpha_Q \tilde{u}^{n+1-Q}}{\Delta t} - \nu \Delta u^{n+1} = f^{n+1} \tag{5}$$

where the α_q are appropriate constants (for example, if $Q = 3$ then $\alpha_0 = \frac{11}{6},\ \alpha_1 = -3,\ \alpha_2 = \frac{3}{2},\ \alpha_3 = -\frac{1}{3}$). As previously mentioned, u^{n+1} is an approximation of $u(x, t)$ at time $t = t^{n+1}$ and, for simplification, we have denoted by $\tilde{u}^{n+1-q},\ q = 1, \ldots, Q$ approximations of $\tilde{u}(x, t^{n+1};\ t^{n+1-q}) := u(\chi(x, t^{n+1};\ t^{n+1-q}), t^{n+1-q})$.

Clearly, once the $\tilde{u}^{n+1-q}$ are known in Equation (5), u^{n+1} results from the resolution of a diffusion-type problem (the diffusion step). But it is easy to show that the calculation of these $\tilde{u}^{n+1-q}$ may result from the resolution of a set of Q advection equations (the transport step).

Lemma 2.1
Given the function $\mathbf{v}$, we have $\tilde{u}(x, t^{n+1};\ t^n) = \bar{u}(x, t^{n+1})$, the solution at $\tau = t^{n+1}$ of the following advection problem:

$$\begin{cases} \dfrac{\partial \bar{u}(x, \tau)}{\partial \tau} = -\mathbf{v}(x, \tau) \cdot \nabla \bar{u}(x, \tau), \quad t^n \le \tau \le t^{n+1} \\ \bar{u}(x, t^n) = u(x, t^n) \end{cases} \tag{6}$$

Proof
Equation (6) is nothing but the material derivation of $\bar{u}$ set equal to zero, so that

$$\frac{\mathrm{d}\bar{u}(\chi(x, t^{n+1};\ \tau), \tau)}{\mathrm{d}\tau} = 0$$

Hence, we have

$$\bar{u}(\chi(x, t^{n+1};\ t^n), t^n) = \bar{u}(\chi(x, t^{n+1};\ t^{n+1}), t^{n+1})$$

That is

$$\tilde{u}(x, t^{n+1};\ t^n) = \bar{u}(x, t^{n+1}) \qquad \square$$

Similarly, it is clear that

$$\tilde{u}(x, t^{n+1};\ t^{n+1-q}) = \bar{u}(x, t^{n+1}), \quad q = 2, \ldots, Q$$

where $\bar{u}(x, t^{n+1})$ is the solution at $\tau = t^{n+1}$ of the following advection problem:

$$\begin{cases} \dfrac{\partial \bar{u}(x, \tau)}{\partial \tau} = -\mathbf{v}(x, \tau)\cdot\nabla\bar{u}(x, \tau), & t^{n+1-q} \le \tau \le t^{n+1} \\ \bar{u}(x, t^{n+1-q}) = u(x, t^{n+1-q}) \end{cases} \tag{7}$$

Remark 2.1
We have assumed that for any values of x in Ω and $\tau \le t$, $\chi(x, t;\ \tau)$ belongs to the domain Ω. This is valid for confined domains, such as for any $x \in \Gamma$, $\mathbf{v}(x)\cdot\mathbf{n}(x) = 0$, where $\mathbf{n}(x)$ denotes the unit outwards normal at point x of the boundary $\Gamma = \partial\Omega$. For open domains, some feet of the characteristics may fall outside the computational domain. This point is discussed in Section 4.

3. SCHEMES FOR THE TRANSPORT STEP

If the $\tilde{u}^{n+1-q}$ were exactly computed, i.e. if the Q auxiliary advection problems

$$\begin{cases} \dfrac{\partial \bar{u}(x, \tau)}{\partial \tau} = -\mathbf{v}(x, \tau)\cdot\nabla\bar{u}(x, \tau), & t^{n+1-q} \le \tau \le t^{n+1} \\ \bar{u}(x, t^{n+1-q}) = u(x, t^{n+1-q}) \end{cases} \tag{8}$$

$q = 1, 2, \ldots, Q$, were exactly solved, then scheme (5) for the diffusion problem would be unconditionally stable. However, in practice we can never obtain the exact values of the $\tilde{u}^{n+1-q}$. In fact, advection problems (8) have to be approximated using a suitable time scheme. Hereafter, we present possible choices for the time discretization of advection problems (8), which may be solved with a sub-time step $\Delta\tau$, such as $\Delta t = M\Delta\tau$, where M is a positive integer. In the case of the Navier–Stokes equations, the velocity field $\mathbf{v}$ is also unknown and so we focus on explicit time schemes. Consequently, stability constraints have to be considered. They depend on the stability region of the time scheme and on the spectrum of the spatial discrete operator (see, for example, Reference [7]).

3.1. Adams–Bashforth schemes

Adams–Bashforth schemes are frequently used in the calculation of the convection term of the Navier–Stokes equations. For advection problems (8), they yield the following generic form:

$$\bar{u}^{m+1} = \bar{u}^{m} - \Delta\tau(\mathbf{v}\cdot\nabla\bar{u})^{*}$$

with

$$(\mathbf{v}\cdot\nabla\bar{u})^* = \begin{cases} \mathbf{v}^{(m)}\cdot\nabla\bar{u}^m & \text{First-order} \\ \dfrac{3}{2}\mathbf{v}^{(m)}\cdot\nabla\bar{u}^m - \dfrac{1}{2}\mathbf{v}^{(m-1)}\cdot\nabla\bar{u}^{m-1} & \text{Second-order} \\ \dfrac{23}{12}\mathbf{v}^{(m)}\cdot\nabla\bar{u}^m - \dfrac{16}{12}\mathbf{v}^{(m-1)}\cdot\nabla\bar{u}^{m-1} + \dfrac{5}{12}v^{(m-2)}\cdot\nabla\bar{u}^{m-2} & \text{Third-order} \end{cases}$$

To begin the iterative procedure, i.e. for $m = 0$, one uses $\bar{u}^0 = u^{n+1-q}$. The iteration number is equal to qM, in such a way that $\tilde{u}^{n+1-q} = \bar{u}^{qM}$. The $\mathbf{v}^{(m)}$ are the values of $\mathbf{v}$ at time $\tau = t^{n+1-q} + m\Delta\tau$. The full Q-order backward Euler/L-order Adams–Bashforth (BEQ/ABL) scheme is formally of order $\min(Q, L)$ in time, as a result of a consistency analysis successively applied to Equations (8) and (5). There is no stability restriction on Δt due to the unconditional stability of the BEQ approximation, but the sub-time step $\Delta\tau$ should be determined from the condition that the spectrum of the spatial discretization of the operator $\Delta\tau\mathbf{v}\cdot\nabla$ belongs to the absolute stability region of the explicit ABL scheme. Note that the spectral Legendre approximation of the first-derivative operator shows imaginary eigenvalues, so that in this case we should choose the AB3 scheme because it is stable along some portion of the imaginary axis. This is no-more true in case of a spectral Chebyshev approximation, where the AB2 scheme should be considered.

Now let us determine $\tilde{u}^n$, $\tilde{u}^{n-1}, \ldots, \tilde{u}^{n+1-q}$ in Equation (5) from the AB1 approximation applied to the sub-problems (8), with the time steps Δt, $2\Delta t, \ldots, Q\Delta t$ respectively, i.e.

$$\frac{\tilde{u}^{n+1-q} - u^{n+1-q}}{q\Delta t} = -\mathbf{v}^{n+1-q}\cdot\nabla u^{n+1-q}, \quad 1 \le q \le Q$$

Then, this approach results in

$$\frac{\sum_{q=0}^{Q} \alpha_q u^{n+1-q}}{\Delta t} - \nu\Delta u^{n+1} = f^{n+1} - (\mathbf{v}\cdot\nabla u)^+$$

where

$$(\mathbf{v}\cdot\nabla u)^+ = \left(\sum_{q=1}^{Q} -q\alpha_q \mathbf{v}^{n+1-q}\cdot\nabla u^{n+1-q}\right)$$

which is exactly the standard Q-order semi-implicit BEQ/ABQ scheme, as can be easily recovered by Taylor developments of $u(x, t^{n+1-q})$, $1 \le q \le Q$, at time t^{n+1}.

Let us emphasize that the notation AB here simply refers to the so-called 'Adams–Bashforth extrapolation' (at time t^{n+1}). For example, one obtains

$$(\mathbf{v}\cdot\nabla u)^+ = \begin{cases} \mathbf{v}^n\cdot\nabla u^n & \text{First-order} \\ 2\mathbf{v}^n\cdot\nabla u^n - \mathbf{v}^{n-1}\cdot\nabla u^{n-1} & \text{Second-order} \\ 3\mathbf{v}^n\cdot\nabla u^n - 3\mathbf{v}^{n-1}\cdot\nabla u^{n-1} + \mathbf{v}^{n-2}\cdot\nabla u^{n-2} & \text{Third-order} \end{cases}$$

3.2. Runge–Kutta schemes

For illustration, we consider the fourth-order Runge–Kutta (RK4) scheme

$$\begin{cases} \text{given } \bar{u}^m \\ R_1 = -\mathbf{v}^{(m)}\cdot\nabla\bar{u}^m \\ R_2 = -\mathbf{v}^{(m+1/2)}\cdot\nabla\left(\bar{u}^m + \dfrac{1}{2}\Delta\tau R_1\right) \\ R_3 = -\mathbf{v}^{(m+1/2)}\cdot\nabla\left(\bar{u}^m + \dfrac{1}{2}\Delta\tau R_2\right) \\ R_4 = -\mathbf{v}^{(m+1)}\cdot\nabla(\bar{u}^m + \Delta\tau R_3) \\ \bar{u}^{m+1} = \bar{u}^m + \dfrac{\Delta\tau}{6}(R_1 + 2R_2 + 2R_3 + R_4) \end{cases} \tag{9}$$

where again the $\mathbf{v}^{(m)}$ are the values of $\mathbf{v}$ at time $\tau = t^{n+1-q} + m\Delta\tau$.

The semi-Lagrangian BEQ/RK4 scheme is formally of order $\min(Q, 4)$ in time. As for the BEQ/ABL, there is no stability restriction on Δt but stability restrictions on $\Delta\tau$. They can be determined from the absolute stability region of the explicit RK4 scheme, together with the discrete spectrum of the operator $\mathbf{v}\cdot\nabla$. Theoretically, the RK4 scheme is more stable than the AB2 or the AB3, due to its larger absolute stability region. This is why it will be used in our numerical experiments (Section 5). However, the RK4 algorithm needs four consecutive gradient operations at each sub-time step, rather than two (or three) for the AB2 (or AB3) scheme.

To conclude this section we apply the semi-Lagrangian BEQ/RK4 scheme to the Navier–Stokes equations

$$\begin{cases} \dfrac{\partial\mathbf{u}}{\partial t} + (\mathbf{u}\cdot\nabla)\mathbf{u} - \nu\Delta\mathbf{u} + \nabla p = 0 \\ \nabla\cdot\mathbf{u} = 0 \end{cases} \tag{10}$$

The BEQ approximation of the material derivative yields the Stokes-like problem

$$\frac{\alpha_0\mathbf{u}^{n+1} + \alpha_1\tilde{\mathbf{u}}^n + \cdots + \alpha_Q\tilde{\mathbf{u}}^{n+1-Q}}{\Delta t} - \nu\Delta\mathbf{u}^{n+1} + \nabla p^{n+1} = 0,$$

$$\nabla\cdot\mathbf{u}^{n+1} = 0$$

where the previous solutions $\tilde{\mathbf{u}}^{n+1-q}$ are computed by solving the Q advection sub-problems

$$\begin{cases} \dfrac{\partial \tilde{\mathbf{u}}(x,\tau)}{\partial \tau} = -\mathbf{u}(x,\tau)\cdot\nabla\tilde{\mathbf{u}}(x,\tau), \quad t^{n+1-q} \le \tau \le t^{n+1} \\ \tilde{\mathbf{u}}(x,t^{n+1-q}) = \mathbf{u}(x,t^{n+1-q}) \end{cases} \tag{11}$$

for $q = 1, 2, \ldots, Q$ using a RK4 scheme. It should be remembered that, for q fixed, $\tilde{\mathbf{u}}^{n+1-q}$ is an approximation of $\tilde{\mathbf{u}}(x, t^{n+1})$ (see Lemme 2.1).

The details of the algorithm, with the sub-time step $\Delta\tau = \Delta t/M$, can be written as follows:

Initialization: $m = 0$, $\tilde{\mathbf{u}}^0 = \mathbf{u}^{n+1-q}$
Step m:

$$\begin{cases} \text{Given } \tilde{\mathbf{u}}^m \\ \mathbf{R}_1 = -\mathbf{u}^{(m)}\cdot\nabla\tilde{\mathbf{u}}^m \\ \mathbf{R}_2 = -\mathbf{u}^{(m+1/2)}\cdot\nabla\left(\tilde{\mathbf{u}}^m + \dfrac{1}{2}\Delta\tau\mathbf{R}_1\right) \\ \mathbf{R}_3 = -\mathbf{u}^{(m+1/2)}\cdot\nabla\left(\tilde{\mathbf{u}}^m + \dfrac{1}{2}\Delta\tau\mathbf{R}_2\right) \\ \mathbf{R}_4 = -\mathbf{u}^{(m+1)}\cdot\nabla(\tilde{\mathbf{u}}^m + \Delta\tau\mathbf{R}_3) \\ \tilde{\mathbf{u}}^{m+1} = \tilde{\mathbf{u}}^m + \dfrac{\Delta\tau}{6}(\mathbf{R}_1 + 2\mathbf{R}_2 + 2\mathbf{R}_3 + \mathbf{R}_4) \end{cases}$$

End: If $m = qM$, let $\tilde{\mathbf{u}}^{n+1-q} = \tilde{\mathbf{u}}^{qM}$, Stop.

Similar notations to previously ones have been used, except that dot products have been replaced by vector–tensor products. Moreover, the $\mathbf{u}^{(m)}$ are only approximate values of $\mathbf{u}$ at time $\tau = t^{n+1-q} + m\Delta\tau$. They must be evaluated by sufficiently high-order extrapolations/interpolations from data at the previous time steps ($\mathbf{u}^n$, $\mathbf{u}^{n-1}$, $\mathbf{u}^{n-2}$, ...), in order to preserve the global accuracy of the semi-Lagrangian scheme.

4. BOUNDARY CONDITIONS FOR THE ADVECTION SUB-PROBLEMS

The advection sub-problems (8) that result from the semi-Lagrangian splitting method may need to be completed with appropriate boundary conditions. In fact, due to the hyperbolicity of the advection equation, boundary conditions are only needed at the inflow part Γ_{in} of the boundary Γ, i.e. such as $\mathbf{v}(x)\cdot\mathbf{n}(x) < 0$. This case corresponds to open flows. For flows in confined geometries, such as $\Gamma_{\text{in}} = \varnothing$, no boundary conditions are needed: Especially, if $\mathbf{v}|_\Gamma = 0$, then explicit schemes like ABL or RK4 yield the correct result on the boundary, $\tilde{u}^{n+1-q} = u^{n+1-q}$.

The case $\Gamma_{in} \neq \varnothing$ is less straightforward and hence has significantly restricted the development of characteristics-like methods. Usage of the same boundary conditions for both the diffusion and transport steps may result in low-order convergence, even if high-order schemes are used for the splitted sub-problems. Indeed, for each $x \in \Gamma_{in}$, the characteristic necessarily traces back into the outside of Ω. Specification of $\bar{u}(\chi(x, t;\ \tau), \tau)$ by the same value as $u(x, \tau)$ on Γ_{in} means that the function $u(x, t)$ is locally extended constantly into the exterior of Ω, which introduces a discontinuity of the gradiant of u except for the case $\nabla \mathbf{u}(x) \cdot \mathbf{n}(x) = 0$. However, in practice, such an assumption is less restrictive than it looks, because the computational domain is generally chosen such that the flow is simple at the inlet part of the boundary (parallel, stationary, ...) and becomes complex inside the domain, e.g. due to the presence of an obstacle.

In different situations, to recover high-order accuracy of the splitting scheme, it is necessary to derive better suited inflow boundary conditions for the advection subproblems. The idea comes from the fact that the Q values of $\bar{u}$, defined in problem (8), on the inflow boundary $x \in \Gamma_{in}$ at time t^{n+1} are nothing but the value of u at times t^{n+1-q}, along the characteristic χ which passes at x at time t^{n+1}. The 'natural' choice for $\bar{u}$ on Γ_{in} must be the one that allows u to pass smoothly via the inflow boundary, in such a way that the gradient of u shows no discontinuity.

These considerations lead us to check a 'no inflow boundary condition' approach for the advection problems. Indeed, the most natural extension of u into the outside of Γ_{in} is obtained using a Taylor development. But this one is in fact automatically achieved by using an explicit scheme without any additional boundary conditions. Thus, the RK4 scheme applied to Equation (6) may be viewed as an approach of Taylor developement of $u(\chi(x, t^{n+1};\ t^n), t^n)$ at x. To see that readily, we rewrite Equation (9) in the following form, assuming $\Delta\tau = \Delta t$ and no extrapolation on $\mathbf{v}^{(m)}$:

$$\tilde{u}^n = \bar{u}^1 = u^n + \Delta t \mathbf{v}^n \cdot \nabla u^n + \frac{1}{2}(\Delta t \mathbf{v}^n \cdot \nabla)^2 u^n + \frac{1}{6}(\Delta t \mathbf{v}^n \cdot \nabla)^3 u^n + \frac{1}{24}(\Delta t \mathbf{v}^n \cdot \nabla)^4 u^n$$

where $(\mathbf{v}^n \cdot \nabla)^k$ denotes operator multiplication. On another hand, the fourth-order Taylor developement of $u(\chi(x, t^{n+1};\ t^n), t^n)$ at x gives

$$\begin{aligned} u(\chi(x, t^{n+1};\ t^n), t^n) &= u(x + \chi(x, t^{n+1};\ t^n) - x), t^n) \\ &= u(x + \delta x, t^n) \text{ [where } \delta x = \chi(x, t^{n+1};\ t^n) - x] \\ &= u(x, t^n) + \delta x \cdot \nabla u(x, t^n) + \frac{1}{2}(\delta x \cdot \nabla)^2 u(x, t^n) + \frac{1}{6}(\delta x \cdot \nabla)^3 u(x, t^n) \\ &\quad + \frac{1}{24}(\delta x \cdot \nabla)^4 u(x, t^n) + O(\delta x)^5 \end{aligned}$$

Furthermore, if a first-order approximation is simply used for δx, then

$$\delta x = \Delta t \mathbf{v}^n$$

and we have

$$u(\chi(x, t^{n+1};\ t^n), t^n) = u(x, t^n) + \Delta t \mathbf{v}^n \cdot \nabla u(x, t^n) + \frac{1}{2}(\Delta t \mathbf{v}^n \cdot \nabla)^2 u(x, t^n) + \frac{1}{6}(\Delta t \mathbf{v}^n \cdot \nabla)^3 u(x, t^n) + \frac{1}{24}(\Delta t \mathbf{v}^n \cdot \nabla)^4 u(x, t^n) + O(\Delta t)^5$$

Thus, the explicit RK4 scheme for the sub-problem (6) is just an approximative form (they are equivalent when $\mathbf{v}$ is constant) of the fourth-order Taylor development of $u(\chi(x, t^{n+1};\ t^n), t^n)$, which equals $\tilde{u}(x, t^{n+1};\ t^n)$. In the case of variable velocity $\mathbf{v}$ and sub-cycling calculation, more detailed but similar analysis can be carried out. Nevertheless, as mentioned below, usage of 'no inflow boundary conditions' makes more severe the stability constraints and consequently affects the main interest of the semi-Lagrangian approach.

5. NUMERICAL RESULTS

The main goal here is to compare the accuracy and stability properties between the semi-implicit and semi-Lagrangian schemes. This is done by considering one-dimensional and multi-dimensional problems, using spectral approximations of different kinds. First we consider one-dimensional problems: two tests are done with the viscous Burger's equation and one with the advection–diffusion equation. For semi-Lagrangian methods of different orders and based on the RK4 algorithm for the transport step, we check the accuracy and also investigate the problem of the inflow boundary conditions. Then we go to a two-dimensional problem, namely the so-called regularized driven cavity problem, which we solve by using a spectral element method. The stability properties of the semi-Lagrangian and semi-implicit methods are compared, using for the latter different forms of the convective term (convective, divergence and skew-symmetric forms). Finally, we compute a three-dimensional flow in a confined cavity, using a Fourier–Chebyshev collocation method. Again we make comparisons of stability but also consider the computational cost, in terms of CPU time and elementary operation counts.

In this section we use the notations: SL for semi-Lagrangian, SI for semi-implicit and again BE for backward Euler, AB for Adams–Bashforth and RK for Runge–Kutta. SL(BE3/RK4) denotes a semi-Lagrangian splitting scheme based on a third-order implicit backward Euler approximation for the diffusion step and on a fourth-order explicit Runge–Kutta scheme for the transport step.

5.1. One-dimensional model problems

5.1.1. Burger's equation with homogeneous Dirichlet boundary conditions. We consider the one-dimensional viscous Burger's equation

$$\frac{\partial u}{\partial t} + u\frac{\partial u}{\partial x} - \nu\frac{\partial^2 u}{\partial x^2} = 0$$

where ν is a positive constant.

The computational domain is taken to be $\Omega =]0, \pi[$ and homogeneous Dirichlet boundary conditions are imposed. In this case, there is no 'inflow'into Ω. It is known (see Reference [8]) that with the initial condition

$$u(x, 0) = \sin(x)$$

the one-dimensional Burger's equation has an exact solution, given by

$$u(x, t) = \frac{4\nu \sum_{n=1}^{\infty} n a_n \, \mathrm{e}^{-\nu n^2 t} \sin(nx)}{a_0 + 2 \sum_{n=1}^{\infty} a_n \, \mathrm{e}^{-\nu n^2 t} \cos(nx)} \tag{12}$$

with

$$a_n = (-1)^n I_n\left(\frac{1}{2\nu}\right)$$

where I_n is the exponentially increasing Bessel function of the second kind. In the calculations we take $\nu = 0.05$. The profile of the exact solution at time $t = 1.0$ is plotted in Figure 1.

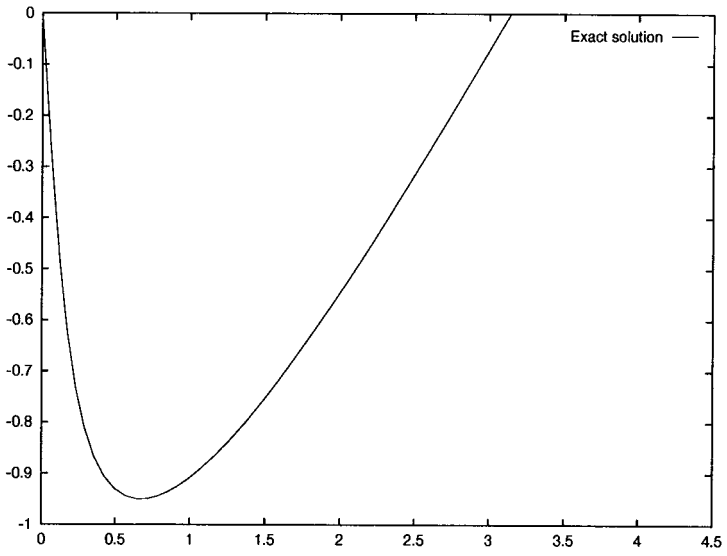

Figure 1. Profile of the exact solution of Equation (12) at $t = 1.0$.

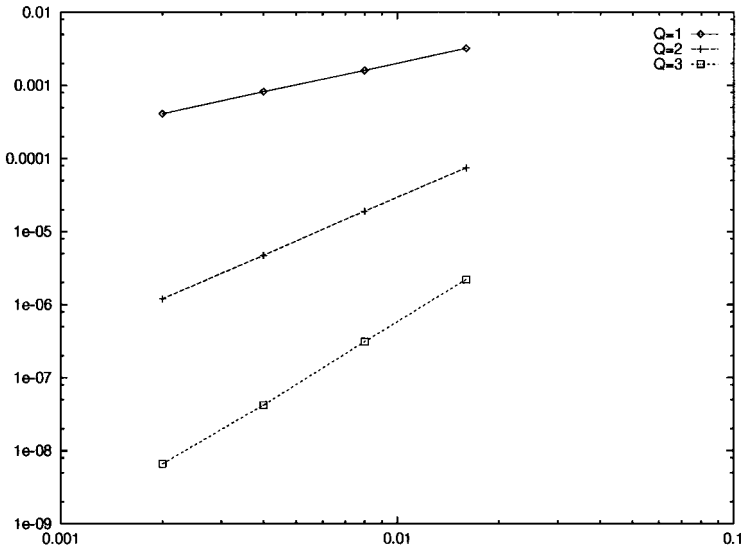

Figure 2. Errors in the L^2-norm at time $t = 1.0$ versus the time step Δt for the solution of Equation (12) of the one-dimensional viscous Burger's problem, using the SL(BEQ/RK4) scheme with $Q = 1$ ($\diamond$), $Q = 2$ ($+$), $Q = 3$ ($\square$).

We first verify the time discretization accuracy of different SL schemes and then make comparisons with standard SI ones. The numerical solutions are calculated until the time $t = 1.0$ with different time steps. In all cases, the spatial approximation consists of $K = 3$ Legendre-based spectral elements with a maximum polynomial degree of $N = 16$. The spatial discretization errors were checked to ensure no spatial contamination of the time discretization errors. Figure 2 shows the errors in the L^2-norm at $t = 1.0$ given by the SL(BEQ/RK4) schemes for $Q = 1$, 2, 3 and different time steps. The results were obtained with $\Delta\tau = \Delta t$, i.e. no sub-cycling was used. As expected, the scheme is Q-order accurate because the leading-order error is determined by the backward differentiation.

The SL(BE3/RK4) and the SI(BE3/AB3) schemes are compared in Figure 3. One notes that the SL scheme gives more accurate results than the SI scheme, probably due to less leading-order error terms for the former: one leading-order error term rather than two. One notes also that the SL scheme yields a time approximation order slightly less than the SI one: the slopes are 2.87 and 3.0 respectively.

5.1.2. Burger's equation with non-homogeneous Dirichlet boundary conditions. This second test considers an exact solution of the one-dimensional Burger's equation, with $\nu = 1.0$, in a domain $\Omega =]0, 1[$

$$u(x, t) = \frac{2}{1 + e^{x - t}} \tag{13}$$

The non-homogeneous Dirichlet boundary conditions and the initial condition are imposed to be consistent with the above exact solution. Now $x = 0$ and $x = 1$ are 'inflow' and 'outflow' points respectively. The solution is again integrated until $t = 1.0$ with different time steps. The polynomial degree is $N = 24$ with no spectral element decomposition. Again the spatial discretization errors have been checked to be sure that they may be neglected compared with the time discretization errors.

Figure 4 shows the errors in the H^1-norm at $t = 1.0$ for the SI(BE3/AB3) and SL(BE3/RK4) schemes, with and without inflow boundary conditions for the advection sub-problems of the SL scheme. It is noted that with 'no inflow boundary condition', the high-order convergence of the splitting scheme is maintained, while the specification of the non-homogeneous Dirichlet boundary condition on the inflow boundary for the advection sub-problems results in worse accuracy. This is in agreement with the previous analysis. Nevertheless, the 'no inflow boundary condition' approach induces stability constraints that are more severe, so that no gain is obtained when using the SL scheme rather than the SI one.

5.1.3. Advection–diffusion equation. Now we consider the one-dimensional advection–diffusion equation

$$\frac{\partial u}{\partial t} + a\frac{\partial u}{\partial x} - \nu\frac{\partial^2 u}{\partial x^2} = f$$

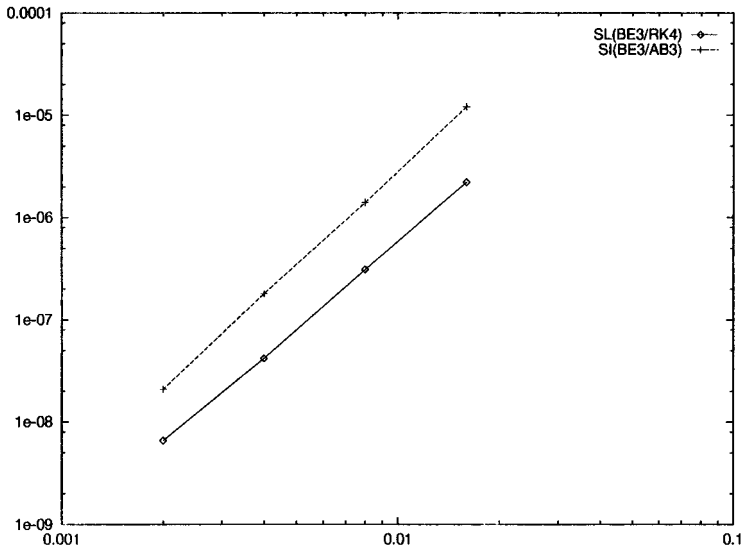

Figure 3. Errors in the L^2-norm at time $t = 1.0$ versus the time step Δt for the solution of Equation (12) of the one-dimensional viscous Burger's problem, using the SL(BE3/RK4) ($\diamond$) and the SI(BE3/AB3) schemes ($+$).

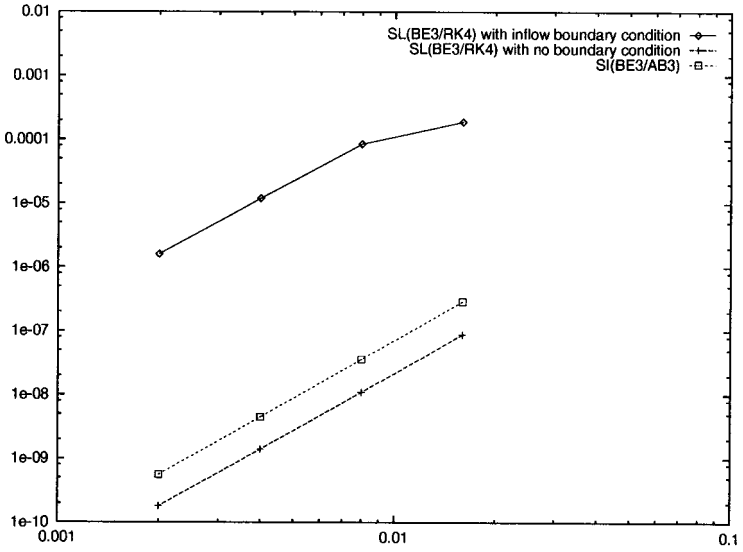

Figure 4. Errors in the H^1-norm at time $t = 1.0$ versus the time step Δt for the solution of Equation (13) of the one-dimensional viscous Burger's problem, for the SL(BE3/RK4), with ($\diamond$) and without ($+$) inflow boundary condition, and for the SI(BE3/AB3) scheme ($\square$).

in the computational domain $\Omega =]0, 1[$ and where a is a positive constant.

For the exact solution we choose the analytical function

$$u(x, t) = x^{\alpha} \frac{2\pi - 1 + \sin(2\pi t)}{2\pi} \sin \pi x \tag{14}$$

where α is a non-negative constant. The Dirichlet boundary conditions and the initial condition are taken consistent with the exact solution. The constant a is fixed to $a = 1$. Figure 5 shows the profile of this exact solution at $t = 1.0$ for various values of α.

For all $\alpha \geq 0$, the solution is vanishing at the two extreme points, $x = 0$ and $x = 1$, which are an 'inflow point' and an 'outflow point' respectively. Here again we can expect that using $x = 0$ the same boundary condition for the diffusion step and the transport step will introduce splitting errors, especially in the case of small α. Indeed, with a constant velocity propagation, the extension of the solution for values of $x < 0$ does not coincide with the homogeneous boundary condition. Nevertheless, one can expect that a zero derivative of the exact solution at the 'inflow point' (this is the case when $\alpha \geq 1$) will limit the splitting errors and even that these errors will decrease when inceasing the parameter α.

The calculations are done with $K = 6$ spectral elements and a maximum polynomial degree $N = 8$. We first compare the stability properties of the SL(BE3/RK4) and SI(BE3/AB3) schemes, as a function of ν, using $\alpha = 2$ (but similar results have been observed for $\alpha = 0$ and $\alpha = 1$). In the present test, no sub-cycling is used, i.e. $\Delta\tau = \Delta t$. Table I lists the critical time

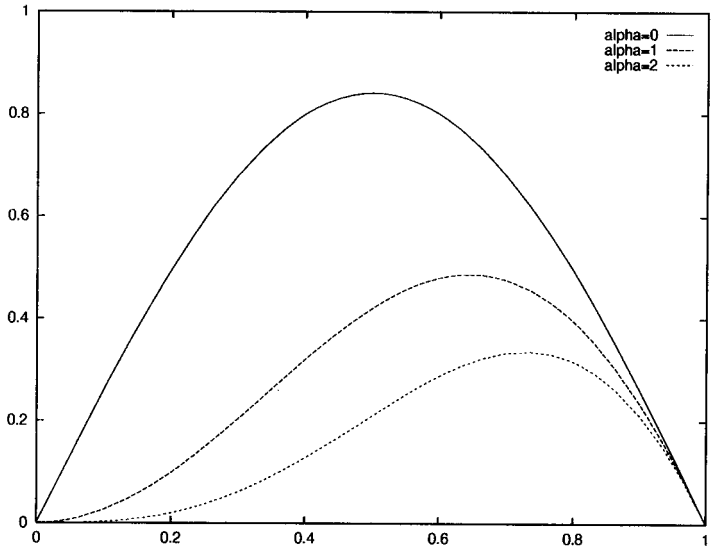

Figure 5. Profile of the exact solution defined by Equation (14) at $t = 1.0$ for $\alpha = 0$, 1, 2.

Table I. Critical time steps for the SL and SI schemes for different values of v ($M = 1$).

v	SI(BE3/AB3) (Δt_c)	SL(BE3/RK4) ($\Delta t'_c$)	Speed-up ($\Delta t'_c/\Delta t_c$)
1.0	Unconditionally stable	0.019 ± 0.001	0.00
0.1	0.07 ± 0.01	0.016 ± 0.001	0.23
0.01	0.007 ± 0.001	0.013 ± 0.001	1.86
0.001	0.0029 ± 0.0001	0.013 ± 0.001	4.48
0.0	0.0026 ± 0.0001	0.011 ± 0.001	4.23

steps $\Delta t'_c$ for the SL scheme and Δt_c for the SI one for different values of the viscosity. The speed-up in the last column is calculated as the ratio of $\Delta t'_c$ and Δt_c. One observes that for large values of the viscosity the SI scheme takes advantage on the SL one: in such cases the diffusion term is dominant and so stabilizes the global schemes. But as expected, when the viscosity decreases, the speed-up resulting from using the SL scheme increases. The maximal speed-up is obtained for $v \approx 0$. Thus, the SL(BE3/RK4) scheme is of interest for small values of the viscosity.

Note that if sub-cycling is used in the solution of the advection sub-problems, then the critical time step of the SL scheme can be increased. For $v = 0.001$ and $\alpha = 2$, Table II shows the influence of the sub-time step number M on stability. As expected, the variation of the critical time step $\Delta t'_c$ with respect to M is essentially linear. We attribute the slight departure from linearity to the fact that $x = 0$ is an inflow point.

Table II. Critical time steps for the SL scheme and speed-up for different values of the sub-time step number M.

M	SL(BE3/RK4) ($\Delta t'_c$)	Speed-up ($\Delta t'_c/\Delta t_c$)
1	0.013 ± 0.001	4.48
2	0.025 ± 0.001	8.62
3	0.036 ± 0.001	12.4
4	0.049 ± 0.001	16.9
8	0.096 ± 0.001	33.1
16	0.190 ± 0.001	65.5

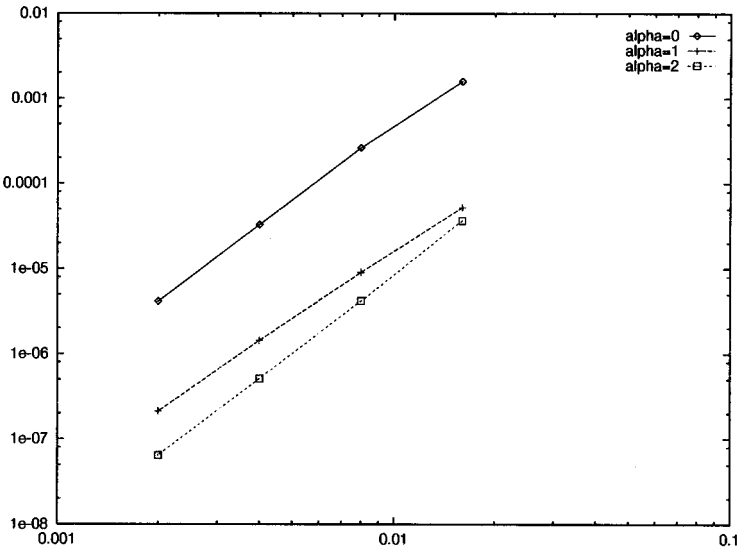

Figure 6. Errors in the L^2-norm at time $t = 1.0$ versus the time step Δt for the solution of Equation (14) of the one-dimensional advection–diffusion equation, with $\alpha = 0$ ($\diamond$), $\alpha = 1$ ($+$) and $\alpha = 2$ ($\square$), using the SL(BE3/RK4) scheme.

For investigations on the accuracy, we test the following three cases: $\alpha = 0,\ 1,\ 2$. Figure 6 shows the time accuracy order for different values of α using the SL(BE3/RK4) scheme in the case $\nu = 0.001$. When $\alpha = 0$, the derivative of the exact solution at the inflow boundary is not zero and so the homogeneous inflow boundary condition is not compatible with the value of the solution along the characteristics. The utilization of this inflow boundary condition results, as mentioned previously, in worse accuracy. But as expected, when α increases, errors stemming from the inflow boundary condition decrease.

In Table III we compare the time errors obtained respectively with the SL(BE3/RK4) and the SI(BE3/AB3) schemes for various values of α and two different time steps in the case $\nu = 0.1$. One observes that the time error of the SL scheme is larger if $\alpha = 0$. However, the SL scheme is more accurate than the SI scheme, as soon as $\alpha \geq 1$.

Table III. Time errors in L^2-norm of the SI and SL schemes for different values of α and for two time steps.

Δt	α	SI(BE3/AB3)	SL(BE3/RK4)
0.0025	0	0.364E−06	0.245E−05
	1	0.198E−06	0.858E−07
	2	0.125E−06	0.428E−07
0.01	0	0.226E−04	0.111E−03
	1	0.127E−04	0.532E−05
	2	0.815E−05	0.184E−05

5.2. Regularized driven cavity problem

The two-dimensional driven cavity problem is considered as a classical test for the Navier–Stokes numerical solvers. The computational domain is $\Omega =]0, 1[^2$, at the initial time the fluid is at rest and we consider for the boundary conditions [9,10], with $\mathbf{u} = (u, v)$

$$u(x, 1, 0) = -16x^2(1-x)^2, \qquad v(x, 1, 0) = 0$$

on the top side and zero on the three other sides, in order to avoid C^0 discontinuities of u in the corners of the cavity. The Reynolds number is defined by $Re = Lu_{\max}/\nu$, where L and $u_{\max}$ are the dimensioned side length and maximum training velocity respectively. Calculations have been carried out for $Re = 400$ and $Re = 1000$. In both cases, the flow converges to a steady state.

The spatial solver is based on the Legendre $\mathbb{P}_N \times \mathbb{P}_{N-2}$ spectral element method (polynomial approximation for the pressure is two degrees less than for the velocity components). The Stokes system is solved by the Uzawa procedure, which splits the resolution process for the pressure and velocity. The pressure system and the velocity system are solved respectively by the outer/inner conjugate gradient iterative algorithm with preconditioning (see References [11–14] for more details).

In the case $Re = 400$, we use $K = 16$ uniform spectral elements and a maximal polynomial degree $N = 16$ in each element and spatial direction. In the case of $Re = 1000$, we take $K = 100$ and $N = 8$. The vorticity (defined as the curl of $\mathbf{u}$) and pressure (up to a constant) fields obtained for this Reynolds number are shown in the Figure 7. Different time schemes are used to perform the computations, in an effort to compare their stability properties. For a given time step Δt, we say that the scheme is stable for this time step if the steady solution is obtained.

We first compare the stability of the SI(BE3/AB3) and SL(BE3/RK4) schemes without sub-time step, i.e. $\Delta\tau = \Delta t$. Then, we vary the number M of the sub-cycles, i.e. we take $\Delta\tau = \Delta t/M$, to determine the maximum time step Δt allowed by the SL scheme for a fixed value of M. Keeping in mind that different discrete forms of the convective term may influence the stability of the SI scheme, comparisons have been performed for the convective, conservative and skew-symmetric forms of this term. Table IV lists the critical time steps. It is noted that the SL scheme allows critical time steps about three times larger than those of the

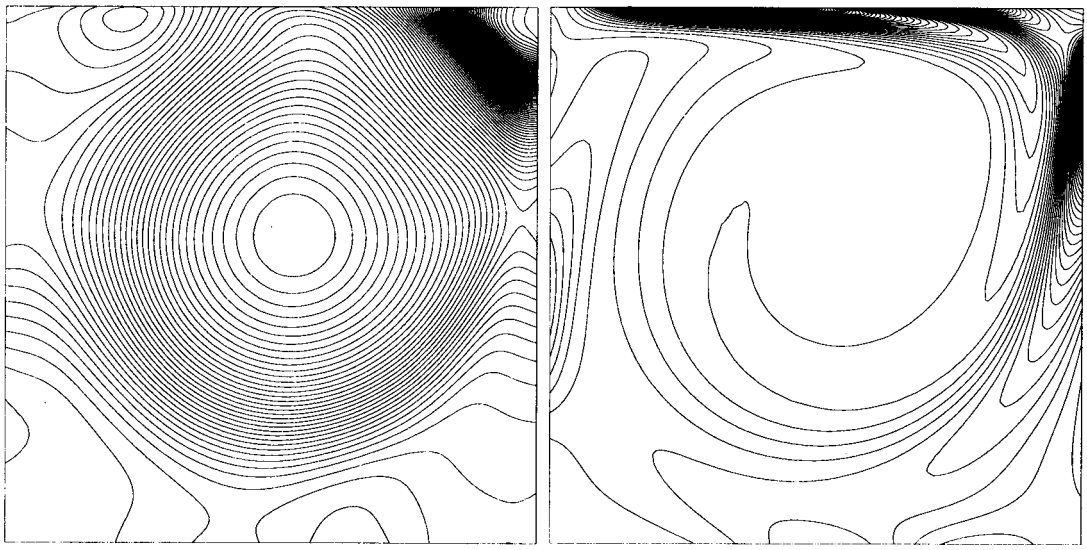

Figure 7. Vorticity and pressure fields for the regularised driven cavity problem at the steady state, $Re = 1000$, $-38.74 \leq \omega \leq 20.86$, $-0.0424 \leq p \leq 0.1223$.

Table IV. Critical time steps for the SL and SI schemes, with different treatments of the convection term.

	SI(BE3/AB3)			SL(BE3/RK4)	
Re	Convect.	Conserv.	Skew-symm.	$\Delta\tau = \Delta t$	$\Delta\tau < \Delta t$
$Re = 400$	0.0040	0.0027	0.0033	0.010	0.070 ($M = 8$)
$Re = 1000$	0.0042	0.0030	0.0036	0.015	0.16 ($M = 11$)

The data are determined with a relative error up to 10 per cent.

standard SI schemes, even without sub-cycling. As previously mentioned, this results from the large absolute stability region of the RK4 algorithm. If sub-cycling is used with $M = 8$ in the case $Re = 400$, the SL scheme allows a critical time step $\Delta t = 0.07$, which is about 18 times larger than those of the SI schemes. In the case $Re = 1000$, if using sub-cycling number $M = 11$, the maximum time step of the SL scheme can reach 0.16 for the SL(BE3/RK4) scheme. This value is 38 times larger than the one obtained with the SI(BE3/AB3) scheme.

5.3. Three-dimensional cavity flow problem

For the comparison of the SL and SI schemes, the definition of the speed-up as the ratio $\Delta t'_c/\Delta t_c$ is only justified if the computation time of the transport step can be neglected. This is generally true, since the diffusion step is treated implicitly, whereas the transport step is treated explicitly. This is still more true for the Navier–Stokes equations, when using the Uzawa

algorithm to solve the Stokes-like problem, as done previously for the two-dimensional regularized driven cavity flow.

When a direct method is used to solve the Stokes problem, or when projection methods are involved, efficient solvers can be developed for the diffusion step. Then, defining the speed-up as the ratio $\Delta t'_c/\Delta t_c$ is no longer justified. This situation is the one met in this section, where it is shown that the SL scheme can still take advantage on the SI one, but in a less convincing way.

The computational domain is the three-dimensional cavity $\Omega =]-0.5, 0.5[^3$ with one periodic direction (z-periodic direction). At the initial time, the fluid is at rest and the three-dimensional flow results from a non-homogeneous Dirichlet condition at the face $x = -0.5$; with $\mathbf{u} = (u, v, w)$

$$v(-0.5, y, z) = (1-4y^2)^2 \sin\left(\pi\left(\frac{z}{0.5}\right)^{1/3}\right), \qquad u(-0.5, y, z) = w(-0.5, y, z) = 0 \tag{15}$$

On the three other faces also parallel to the z-axis, no-slip conditions are considered.

The approximation in the z-periodic direction makes use of a Fourier method, in such a way that at each time step one has to solve a set of two-dimensional Stokes problems. To this end we use a $\mathbb{P}_N \times \mathbb{P}_N$ (polynomials of same degree for the pressure and the velocity components) Chebyshev collocation method. We first solve a Poisson equation for the pressure and then elliptic Helmholtz equations for the velocity components. An influence matrix technique is used to determine the boundary conditions for the pressure, in such a way that the resulting velocity field is perfectly divergence-free (see Reference [15] for more details). For the spatial discretization we use a $61 \times 61 \times 60$ grid, i.e. $N = 60$ in the x- and y-directions and 30 Fourier modes.

For the advection sub-problems, appropriate boundary conditions are *a priori* needed at the two faces orthogonal to the z-periodic direction, since there is flow entering into the cubic domain through these faces. This would be especially complex, since the inflow and outflow parts of the boundary may be time-dependent. However, a simple analysis shows that the Fourier first-derivative operator has only imaginary eigenvalues, as a result, RK4 scheme applied to the corresponding one-dimensional model problem may be stable for both negative and positive velocity, so that no boundary conditions are in fact required. This was furthermore confirmed by our numerical experiences.

The computations are carried out for a Reynolds number $Re = 10000$, where Re is as previouly based on the maximum of the velocity at the training face and on the side-lenght of the cubic cavity. The resulting flow is such that no steady state is reached, i.e. the flow remains unsteady. The comparison of the SL and SI schemes is performed starting from the same initial condition, i.e. the state obtained at $t = 25$ with the SI-based code. Figure 8 shows isosurfaces obtained for the levels $u = \pm 0.02$ of the u-component of the velocity.

We compare the stability properties of the SI(BE2/AB2) and SL(BE2/RK4) schemes. The critical time steps are found to be $\Delta t_c = (0.64 \pm 0.01) \times 10^{-2}$ and $\Delta t'_c = (3.4 \pm 0.1) \times 10^{-2}$ respectively. Thus the ratio $\Delta t'_c/\Delta t_c$ approximately equals 5.31.

Accuracy comparisons are difficult to perform, since the exact flow is not known. Nevertheless, one may expect that for a given time step the SL scheme is slightly more accurate, due to

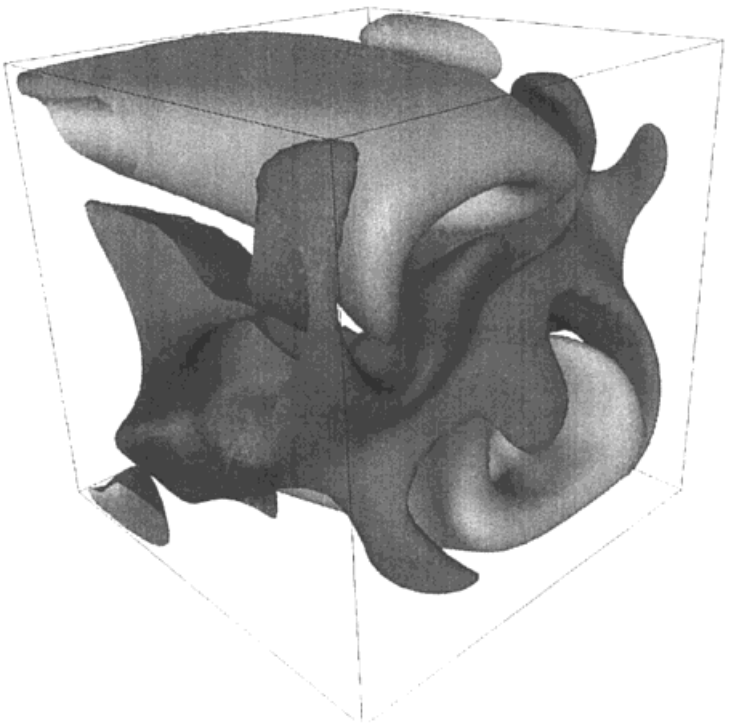

Figure 8. Isosurfaces $u = \pm 0.02$ of the u-component of the velocity for the three-dimensional cavity flow problem, $t = 25$, $Re = 10000$.

the presence of only one leading error term rather than two for the SI scheme. However, in order to take advantage of the SL scheme, a five times larger time step has to be used, resulting in a loss of time accuracy of about 25.

As mentioned above, a comparison of the computational costs of the two schemes does not reduce here to the ratio of the critical time steps: the speed-up must take into account the fact that the SL scheme is more time-consuming than the SI one. This is why we first evaluate the numbers of elementary operations and then confirm these evaluations with CPU time measurements. For three-dimensional problems, the calculation of the convective term with the SI scheme requires 3×3, i.e. 9, velocity component differentiations, at each time step, while the SL one requires $3 \times 4 \times 9$, i.e. 108, differentiations. Hence, the total operation numbers needed to treat the convection term are about $9N^4$ for the SI scheme and $108N^4$ for the SL scheme. The resolution of the Stokes-like problem with the present direct method is estimated to need $34N^4$ operations. Therefore, the total cost at each time step is $9N^4 + 34N^4$ for the SI scheme and $108N^4 + 34N^4$ for the SL scheme. The speed-up obtained from using the SL scheme is then

$$\frac{9N^4 + 34N^4}{108N^4 + 34N^4} \times 5.31 = 1.61$$

With a SGI-R10000 workstation, the CPU time to compute the convection term at each time step is about 2 s by the SI(BE2/AB2) scheme, to be compared with 22 s by the SL(BE2/RK4) scheme. The ratio equals 11, which is in satisfactory agreement with the previous evaluation, $108/9 = 12$. The resolution of the Stokes-like problem needs about 8 s.

The realized speed-up is therefore

$$\frac{2\ \text{s} + 8\ \text{s}}{22\ \text{s} + 8\ \text{s}} \times 5.31 = 1.77$$

All the above results have been obtained without sub-cycling in the advection sub-problems. If sub-cycling is used, the speed-up can be further increased. For example, with $M = \Delta t/\Delta\tau = 2$, the critical time step reaches 0.066, and 41 s are now required by the RK4 algorithm. In this case, the effective speed-up is

$$\frac{2\ \text{s} + 8\ \text{s}}{41\ \text{s} + 8\ \text{s}} \times \frac{0.066}{0.0064} = 2.10$$

However, one may now expect a loss of two orders of magnitude in the time accuracy of the calculation.

6. CONCLUSION

The direct numerical simulation of high-Reynolds number flows remains a challenge for the numerical methods, due to the severe stability constraints induced by the non-linear convective term. The classical characteristics method allows to relax these constraints, but is too much CPU time-consuming in the framework of spectral method. This is why semi-Lagrangian methods, which do not require high-order interpolations, are attractive. Then it was of interest to make comparisons with the standard semi-implicit methods. In all the considered cases, semi-Lagrangian schemes based on backward differentiation for the diffusion step and fourth-order Runge–Kutta method for the transport step, have permitted a non-negligible speed-up, in comparison with semi-implicit schemes based on backward Euler differentiation and Adams–Bashforth extrapolation. Nevertheless, improvements of the explicit scheme used for the transport step, in terms of stability properties and computational cost (see, for example, Reference [16]), would permit to still increase the speed-up, especially when the calculation time of the convective term cannot be neglected.

ACKNOWLEDGMENTS

The authors would like to thank R. Peyret for useful suggestions and also J.M. Lacroix for his helpful technical support. This work was done when C. Xu was in residence at the Laboratoire J.A. Dieudonné, Université de Nice-Sophia Antipolis, France.

REFERENCES

1. Bengué JP, Ibler B, Keramsi A, Labadie G. A new finite element method for Navier–Stokes equations coupled with a temperature equation. In *Proceedins of the 4th International Symposium on Finite Elements in flow Problems*, Kawai T (ed.). North-Holland: Amsterdam, 1982; 295–301.
2. Douglas J, Russell TF. Numerical method for convection dominated diffusion problems based on combining the method of characteristics with finite element or finite difference procedures. *SIAM Journal of Numerical Analysis* 1982; **19**(5): 871–885.
3. Ewing RE, Russell TF. Multistep Galerkin methods along characteristics for convection–diffusion problems. In *Advances in Computer Methods for Partial Differential Equations-IV*, Vichnevetsky R, Stepleman RS (eds). IMACS, Rutgers University: New Brunswisk, NJ, 1981; 28–36.
4. Pironneau O. On the transport–diffusion algorithm and its applications to the Navier–Stokes equations. *Numerische Mathematica* 1982; **38**: 309–332.
5. Boukir K, Maday Y, Métivet B. A high order characteristic method for the incompressible Navier–Stokes equations. *Computer Methods in Applied Mechanics and Engineering* 1994; **116**: 211–218.
6. Maday Y, Patera AT, Ronquist EM. An operator-integration-factor splitting method for time-dependent problems: application to incompressible fluid flow. *Journal of Scientific Computing* 1990; **5**(4): 263–292.
7. Canuto C, Hussaini MY, Quarteroni A, Zang ZA. *Spectral Methods in Fluid Dynamics*. Springer: New York, 1987.
8. Benton ER, Platzman GW. A table of solutions of the one-dimensional Burgers equation. *Quarterly of Applied Mathematics* 1972; **2**: 195–212.
9. Bourcier M, François C. Intégration numerique des équations de Navier–Stokes dans un domaine carré. *Recherche Aérospatiale* 1969; **131**: 23–33.
10. Peyret R, Taylor TD. *Computational Methods for Fluid Flow*. Springer: New York, 1983.
11. Maday Y, Meiron D, Patera AT, Ronquist EM. Analysis of iterative methods for the steady and unsteady Stokes problem: application to spectral element discretization. *SIAM Journal of Scientific Computing* 1993; **14**(2): 310–337.
12. Maday Y, Patera AT. Spectral element methods for the Navier–Stokes equations. In *State-of-the-Art Surveys in Computational Mechanics*, Noor AK (ed.). ASME: New York, 1988; 71–143.
13. Ronquist EM. Optimal spectral element methods for the unsteady three-dimensional incompressible Navier–Stokes equations. PhD thesis, Massachusetts Institute of Technology, 1988.
14. Xu CJ, Maday Y. A global algorithm in spectral method for viscous/inviscid coupling. *Chinese Annual of Mathematics (B)* 1997; **18**(2): 191–200.
15. Sabbah C, Pasquetti R. A divergence-free multi-domain spectral solver of the Navier–Stokes equations in geometries of high aspect ratio. *Journal of Computational Physics* 1998; **139**: 359–379.
16. Carpenter MH, Kennedy CA. A fourth-order 2N-storage Runge–Kutta scheme. NASA TM 109112, 1994.

